JLAB USER GROUP

Jefferson Lab PAC16
Proposal Cover Sheet

This document must be received by close of business Thursday, June 8, 1998 at:

Jefferson Lab
User Liaison,
Mail Stop 12B
12000 Jefferson Ave.
Newport News, VA
23606

Experimental Hall: C

Days Requested for Approval: 7

❒ Proposal Title:

F_2^N at Low Q^2

Proposal Physics Goals

Indicate any experiments that have physics goals similar to those in your propos

Approved, Conditionally Approved, and/or Deferred Experiment(s) or proposals:

None

Contact Person

Name: CHRIS ARMSTRONG
Institution: JEFFERSON LAB
Address: 12000 JEFFERSON AVE
Address: MS 12H
City, State, ZIP/Country: NEWPORT NEWS, VA 23606 USA
Phone: 757-269-7168 Fax: 757-269-5235
E-Mail: csa@jlab.org

Jefferson Lab Use Onl

Receipt Date: 12/14/99 PR 00-002

By: [redacted]

BEAM REQUIREMENTS LIST

JLab Proposal No.: _____ Date: _____

Hall: C Anticipated Run Date: _____ PAC Approved Days: _____

Spokesperson: CHRIS ARMSTRONG Hall Liaison: Rolf Ent
Phone: 757-269-7168
E-mail: csa@jlab.org

List all combinations of anticipated targets and beam conditions required to execute the experiment. (This list will form the primary basis for the Radiation Safety Assesment Document (RSAD) calculations that must be performed for each experiment.)

Condition No.	Beam Energy (MeV)	Mean Beam Current (μA)	Polarization and Other Special Requirements (e.g., time structure)	Target Material (use multiple rows for complex targets — e.g., w/windows)	Material Thickness (mg/cm²)	Est. Beam-On Time for Cond. No. (hours)
1	4400	50	None	LH2	0.29	30
				Al	0.11	30
2	4400	50		LD2	0.65	30
				Al	0.11	30
3	4400	30		Al	0.50	11
4	3300	50		LH2	0.29	14
				Al	0.11	14
5	3300	50		LD2	0.65	14
				Al	0.11	14
6	3300	30		Al	0.50	6
7	2200	50		LH2	0.29	12
				Al	0.11	12

The beam energies, E_{Beam}, available are: $E_{Beam} = N \times E_{Linac}$ where N = 1, 2, 3, 4, or 5. E_{Linac} = 800 MeV, i.e., available E_{Beam} are 800, 1600, 2400, 3200, and 4000 MeV. Other energies should be arranged with the Hall Leader before listing.

cont'd on next page

BEAM REQUIREMENTS LIST

JLab Proposal No.: _____ Date: _____

Hall: _____ Anticipated Run Date: _____ PAC Approved Days: _____

Spokesperson: _____ Hall Liaison: _____
Phone: _____
E-mail: _____

Continued from last page

List all combinations of anticipated targets and beam conditions required to execute the experiment. (This list will form the primary basis for the Radiation Safety Assesment Document (RSAD) calculations that must be performed for each experiment.)

Condition No.	Beam Energy (MeV)	Mean Beam Current (μA)	Polarization and Other Special Requirements (e.g., time structure)	Target Material (use multiple rows for complex targets — e.g., w/windows)	Material Thickness (mg/cm²)	Est. Beam-On Time for Cond. No. (hours)
8	2200	50		LD2	0.65	12
				Al	0.11	12
9	2200	30		Al	0.50	4

The beam energies, E_{Beam}, available are: $E_{Beam} = N \times E_{Linac}$ where N = 1, 2, 3, 4, or 5. E_{Linac} = 800 MeV, i.e., available E_{Beam} are 800, 1600, 2400, 3200, and 4000 MeV. Other energies should be arranged with the Hall Leader before listing.

LAB RESOURCES LIST

JLab Proposal No.: _____ Date _____

(For JLab ULO use only.)

List below significant resources — both equipment and human — that you are requesting from Jefferson Lab in support of mounting and executing the proposed experiment. Do not include items that will be routinely supplied to all running experiments such as the base equipment for the hall and technical support for routine operation, installation, and maintenance.

Major Installations *(either your equip. or new equip. requested from JLab)*

New Support Structures:

Data Acquisition/Reduction

Computing Resources:

New Software:

Major Equipment

Magnets:

Power Supplies:

Targets:

Detectors:

Electronics:

Computer Hardware:

Other:

Other: Need low-profile pipe to beam dump to allow HMS operation at 10.5 deg (as configured during E93-021)

Computing Requirements for F_2^N at Low Q^2

C. Armstrong

December 14, 1999

- Raw Data: ≈250 GB.
- Computer resources for reconstruction and analysis: ≈15,000 SPECint95 hours.
- Computer resources for simulations: ≈15,000 SPECint95 hours.
- On-line disk space: ≈80 GB.
- No foreseen need to transfer data to other institutions.
- No other special requirements.

F_2^N at low Q^2

December 14, 1999

Submitted by

C. S. Armstrong (spokesperson), R. Ent, K. Garrow, A. Lung, D. J. Mack, J. Mitchell, S. A. Wood
Jefferson Lab, Newport News, VA

I. Niculescu (spokesperson)
The George Washington University, Washington, DC

D. Meekins
Florida State University, Tallahassee, FL

H. Bitao, M. E. Christy, A. Cochran, P. Guèye, C. Jackson, C. E. Keppel
Hampton University, Hampton, VA

G. Niculescu
Ohio University, Athens, OH

P. Stoler
Rensselaer Polytechnic Institute, Troy, NY

E. Kinney
The University of Colorado at Boulder, Boulder, CO

R. Asaturyan, H. Mkrtchyan, S. Stepanyan, V. Tadevosyan
Yerevan Physics Institute, Armenia

F_2^N at low Q^2

Abstract

We propose to extend measurements of the proton and neutron structure functions, F_2^p and F_2^n, to low Q^2 and moderately low Bjorken x, into a regime where there is presently little data on these fundamental quantities. In addition, recent work suggests that in the low Q^2, low x regime, F_2^p drops quickly with decreasing momentum transfer, which can be interpreted as an insensitivity to the quark component of the nucleon sea. We will investigate this phenomenon and, utilizing quark-hadron duality, explore to what extent this effect occurs at low Q^2 but moderate x.

1 Introduction

The structure functions F_2^N are quantities fundamental to our understanding of physics at the nucleon scale. Over a broad range in momentum transfer Q^2 and Bjorken x, these quantities are well measured. Fig. 1 shows a set of F_2^p data representative of the world's data in this regime plotted as a function of Q^2, binned in x. Over the large range in Q^2 shown, and especially at higher Q^2, the structure of the data in each x bin is well understood in terms of logarithmic scaling violations. Here, perturbative quantum chromodynamic (PQCD) calculations of leading order (LO) and next-to-leading order (NLO) terms together with target mass corrections reproduce the data very well. At values of x from 0.01 to about 0.2, however, there are almost no data in the region $Q^2 < 0.7$ GeV^2.[1]

Fig. 2 shows a diagram of Q^2 versus ν in the region generally accessible to Hall C at Jefferson Lab. The resonance region is bounded by the two lines of constant invariant mass, $W^2 = m_p^2$ and $W^2 = 3.5$ GeV^2. Lines of constant x emanate from the origin. The light shaded bands on the lines of constant x denote the regions where precise F_2^N data currently exist. While the structure function data generally extend down to the resonance region for $x > 0.14$, there is a paucity of data at low Q^2 and low x.[2]

The dark shaded bands on the lines of constant x indicate where we propose to measure the proton and neutron structure functions. The objective of the proposed experiment is to map out F_2^N in both the low Q^2, low x ($W^2 > 3.5$ GeV^2) region where there is presently little data, and in the the low Q^2, moderate x (resonance) region (using a quark-hadron duality approach for the latter). Recent Jefferson Lab work indicates that in both of these regimes we are seeing the onset of a transition in F_2^p with decreasing Q^2 [Nic99]. In one interpretation, the two results together could yield information about the coherence length of $q\bar{q}$ pairs in the sea.

2 Motivation

In Fig. 3 we show a plot similar to Fig. 1, but zoomed in on the low Q^2 region. The existing precision data, which in most cases extend down to a four-momentum transfer of roughly 0.7 (GeV/c)^2, are shown as a light band for each x bin (the width of the band is indicative of the uncertainties in the data). In addition, we show several individual data points at $x \approx 0.07$, described below:

[1] The data at $x > 0.2$ extend down in Q^2 all the way to the resonance region.

[2] Note that there exist data at low Q^2 and *very* low x from E665 [Ada96a], H1 [Abt93, Ahm95, Aid96, Adl97], NMC [Arn97], and ZEUS [Der93, Der95a, Der95b, Der96, Bre97, Bre98], but these data are at energy losses much greater than those we are considering here.

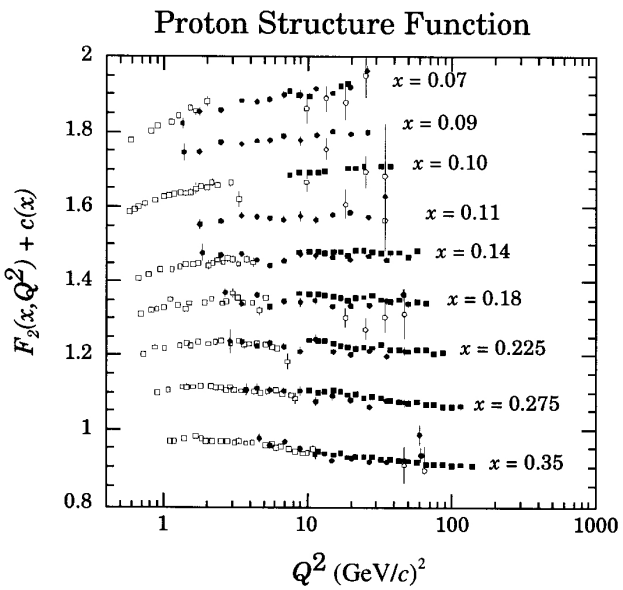

Figure 1: Representative data for F_2^p (from E665 [Ada96b], H1 [Aid96, Adl97], and ZEUS [Der96, Bre97]), shown as a function of Q^2. For plotting clarity, each x bin is offset by a constant. This figure is taken from Ref. [Cas98].

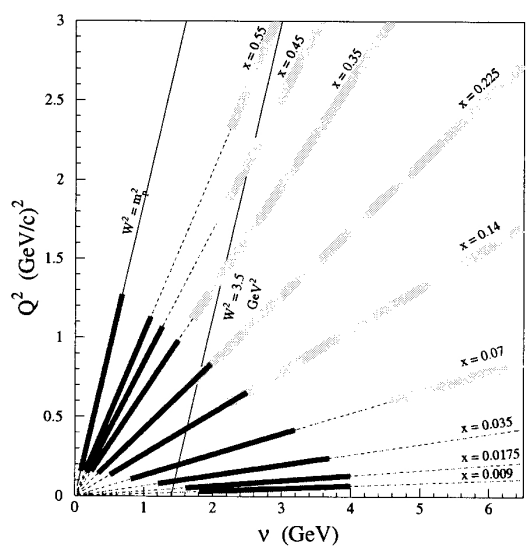

Figure 2: Q^2 versus ν. The resonance region is in between the lines of constant W^2 ($W^2 = m_p^2$ and $W^2 = 3.5$ GeV^2). Lines of constant x are shown, with light bands indicating existing data. The dark bands along lines of constant x indicate the kinematic region over which we propose to measure F_2^p and F_2^n.

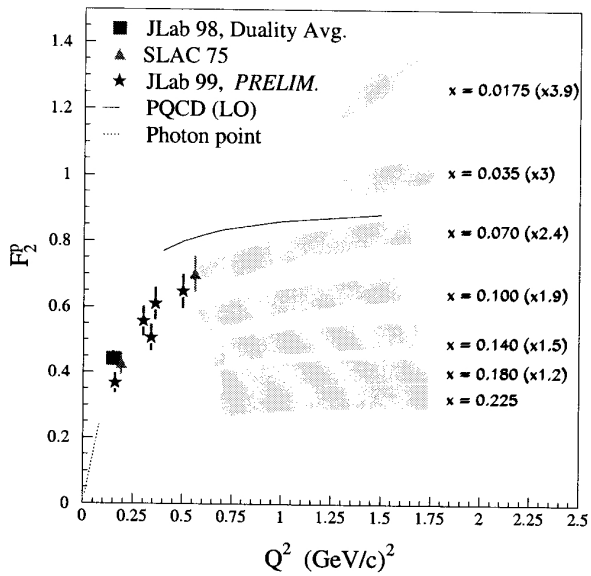

Figure 3: F_2^p as a function of Q^2 in the low Q^2 region. The light bands at constant x are representative of the world's data.

- The square datum is from a study of quark-hadron duality based on recent data from Hall C at Jefferson Lab [Nic98, Nic99]. The point was taken from a scaling curve obtained by averaging inclusive scans in the resonance region, and is from a region where duality holds well (thus higher twist effects appear to be small or cancelling).
- The two triangles are from a SLAC experiment performed in the 1970s [Ste75], and they generally confirm the trend indicated by the duality approach.
- The stars are preliminary results from a few brief test runs taken in Hall C in the summer of 1999 (at different kinematics than the SLAC data). While there are still large systematic uncertainties associated with this data set (reflected in the errors bars), it does confirm that F_2^p is decreasing rapidly with decreasing Q^2.

Note that the good agreement between the three data sets at low Q^2 indicates that higher twist effects are not playing a large role here. The thin solid line shows the evolution (LO) at $x = 0.07$ expected from PQCD. The low Q^2 data described above not only show violations from scaling, but are *clearly deviating from the expected Q^2 evolution* in a region where higher twist effects do not appear to be substantial.

The dashed line shows a sample $F_2 \propto Q^2$ curve, a condition that is required by gauge invariance at the photon point. While the low Q^2 data do not obey the expected evolution, they also do not yet have the slope implied by the photon point requirement.

We can view this 'turn off' of F_2^p in another context, with interesting implications. The Bloom-Gilman (quark-hadron) duality study referenced above has led to the following observation: the curve of F_2^p obtained by averaging inclusive scans in the resonance region (a so called 'scaling curve') has a shape very similar to the well-known xF_3 data set – see Fig. 4. Recall that to first order, xF_3 is sensitive to *valence structure only.* The F_2 curve shown in Fig. 4 is in striking contrast with the usual picture of F_2 obtained from deep inelastic scattering (DIS) experiments and associated parameterizations (NMC [Arn95], MRS [Mar94],

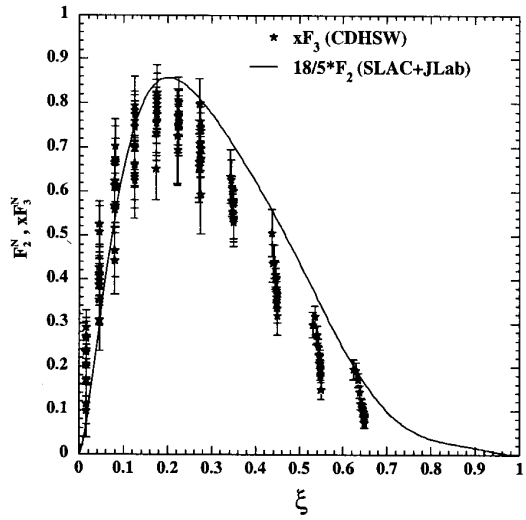

Figure 4: The data are xF_3 as a function of ξ (ξ can be considered as Bjorken x with corrections for target mass effects; the two quantities are essentially the same at low x). The line shows F_2 derived from a duality study of the resonance region, which at low x is sensitive to low Q^2. The F_2 curve has been adjusted by a factor of 18/5 to account for quark charges. This figure is from Ref. [Nic98].

CTEQ4 [Lai97]), which has F_2 *rising* with decreasing x, reflecting large contributions from the nucleon sea. In other words, the duality data (which, in contrast to DIS data, probe *low* Q^2 at low x) suggest that in this regime, F_2^p may be sensitive to valence structure only. The goal of this proposal is to study the structure functions $F_2^{n,p}$ in this region where F_2^p drops off.

We can see from Fig. 5 that the fall off of F_2^p seen in the Jefferson Lab duality study is consistent with data from other experiments probing significantly lower x. The three plots in the figure show F_2^p as a function of x for three different values of Q^2, together with the parameterization from the GRV collaboration [Glu95, Glu98]. At low x, the structure function F_2^p depends very strongly on Q^2. This is consistent with the conclusion from the Jefferson Lab data: *for fixed x, as we move to lower momentum transfer, we see an apparent drop-off of the nucleon sea.* There has also been long-standing debate about how low in Q^2 we will be able to make reasonable use of the parton model. The GRV curves in Fig. 5 indicate that this particular version of the model works surprisingly well even down to the $Q^2 \approx 1$ (GeV/c)^2 range, although by $Q^2 \approx 0.3$ GeV/c)^2 it is breaking down.[3]

The kinematics proposed in this experiment would extend the existing Jefferson Lab data down significantly in both Q^2 and x, in the region where a drop off in F_2 has been observed and the parton model appears to be failing. One of our objectives is to learn how the Q^2 dependence of the structure functions at low x relates to that at higher x (where we expect to be dominated by valence structure). The proposed experiment also includes some data in the resonance region. This will allow us to explore the nucleon structure functions at low Q^2 but moderate x (namely, in the resonance region) using quark-hadron duality. The Jefferson Lab duality study has shown that local duality (individual resonant peaks averaging to the DIS scaling curve) holds quite well even down to small momentum transfers [Nic98, Nic99].[4] If we assume that

[3]The GRV model uses parton distributions evolved from $Q^2 = 0.4$ (GeV/c)^2.

[4]The JLab work indicates that local duality holds at the several percent level above $Q^2 = 1$ (GeV/c)^2, and roughly at the 10% level at $Q^2 = 0.5$ (GeV/c)^2. Future analysis is planned to determine these levels of agreement more precisely.

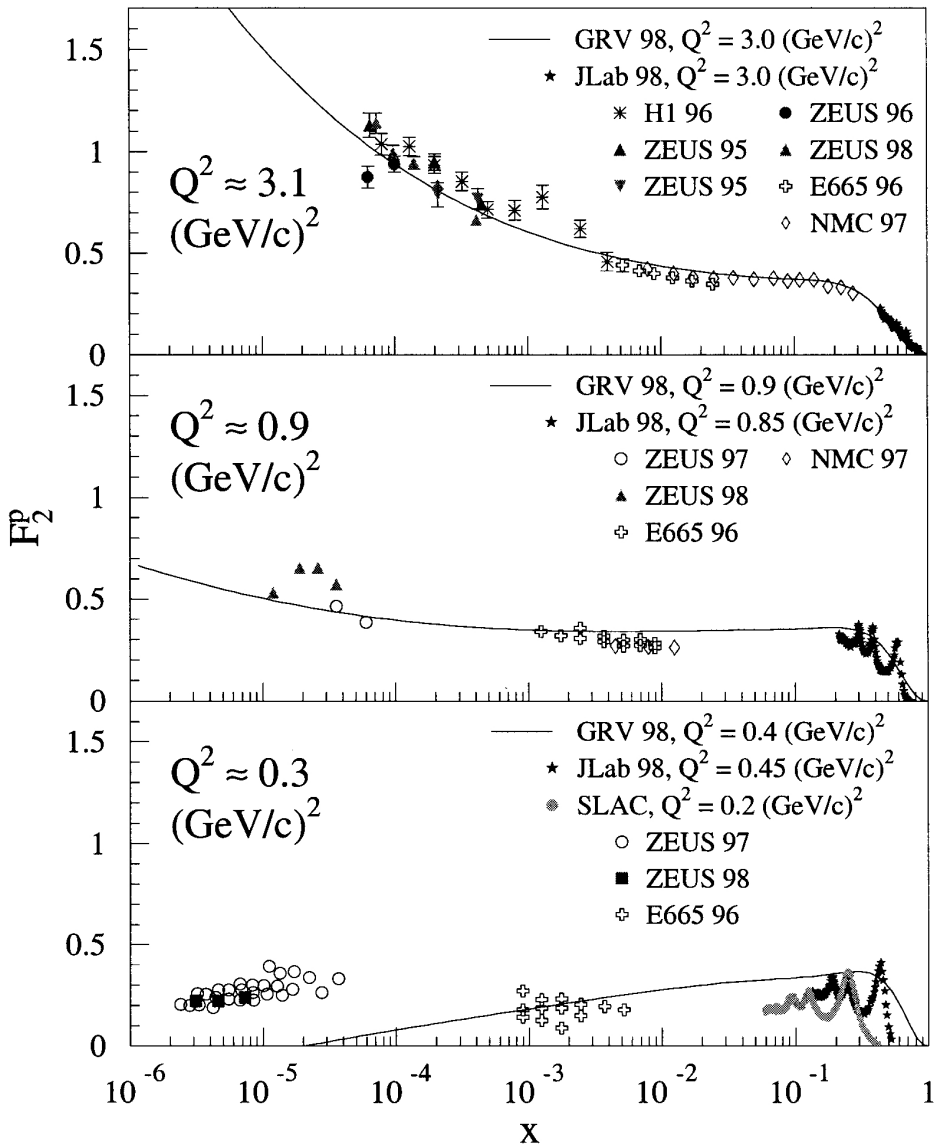

Figure 5: F_2^p as a function of x for three values of Q^2, with a logarithmic x scale. The proposed experiment would extend the Jefferson Lab data down to $x = 0.01$ at $Q^2 \approx 0.03$ (GeV/c)^2.

E_b (GeV)	θ_e (deg.)	E' (GeV)	x	Q^2 (GeV/c)^2	ε
4.4	16.0	0.4–3.9 (22 settings)	0.016–1	0.13–1.42	0.18–0.95
4.4	10.5	0.4–3.9 (22 settings)	0.007–1	0.05–0.61	0.18–0.98
3.3	10.5	0.4–3.1 (20 settings)	0.007–1	0.04–0.36	0.24–0.98
2.2	10.5	0.4–2.2 (17 settings)	0.008–1	0.03–0.16	0.35–0.98

Table 1: Kinematics for the proposed experiment. Data will be taken with ^{1}H, ^{2}H, and Al (dummy) targets.

local duality holds, *we can use resonance-averaged measurements to extract information about the behavior of F_2 in kinematic regions otherwise inaccessible.*

Finally, we are also interested in finding out how the structure functions behave as we increase x at low Q^2. As pointed out above, one interpretation of the Jefferson Lab inclusive data is that F_2 is insensitive to the nucleon sea at low Q^2. In other words, as we increase the wavelength of the probe, it will at some point fail to resolve $q\bar{q}$ pairs in the nucleon. By looking at the structure functions at low Q^2 as a function of x, we hope to shed light on this situation and possibly learn about the coherence length of $q\bar{q}$ pairs in the sea.

3 The Experiment

This experiment will use the HMS together with the standard 4 cm cryogenic target cells filled with ^{1}H and ^{2}H liquids. In order to access the lowest x and Q^2 proposed, the HMS will need to reach 10.5 degrees. The HMS has been used at this angle before (during E93-021, The Charged Pion Form Factor), but reaching it again will require reinstallation of a low-profile beam pipe downstream of the target. Other than this, no special hardware or beam conditions are required.

Because the SOS cannot reach large momenta and because the HMS and SOS cannot simultaneously be at very small angles, all primary data in this experiment will be taken with the HMS. The SOS will be used to perform auxiliary scans and to monitor the luminosity.

Table 1 gives the kinematics proposed for the experiment. We plan to perform cross section measurements of systematic uncertainty of about 3%, which has been previously achieved in Hall C and which easily satisfies the physics goals of the experiment. The ratio of longitudinal-to-transverse cross sections, R, is necessary to extract F_2 from the experimentally measured cross section. When the results of a recent measurement (E94-110, A Measurement of $R = \sigma_L/\sigma_T$ in the Nucleon Resonance Region) become available, the uncertainty introduced by this quantity should be less than 1%.

Over the kinematic range proposed, the rates are very high – 1 kHz and greater for beam currents around 10 to 50 μA – so even quick runs obtain 1% statistics with 10 MeV binning. Much of the running time will be spent making target and HMS momentum changes. For the beam time request, we assumed runs of 15 minutes, together with 25 minutes per HMS momentum change and 10 minutes per target change. Estimates based on parameterizations of data indicate that π-to-e ratios are roughly 10 at the lowest-momentum kinematics. Using the HMS Čerenkov and shower counters, pion rejection of over 1000 is routine, so pions pose no problem. Table 2 gives the beam time requested for the experiment.

Activity	Time (hours)
Data acquisition	68
Configuration changes	70
Beam energy changes	18
Checkout	12
Total	**168 (7 days)**

Table 2: Beam time request for the proposed experiment.

4 Summary

We request 7 days of beam time in Jefferson Lab Hall C in order to conduct an investigation of the nucleon structure functions F_2^p and F_2^n at low Q^2 and moderately low x, where they are currently not well measured. The measurement is of value not only because these are quantities fundamental to our understanding of physics, but also because it appears that the structure functions may be undergoing a transition in this kinematic domain. The resonance-region data will also be a valuable addition to the Jefferson Lab inclusive data, which has yielded some very interesting studies on Bloom-Gilman duality.

The experiment requires no special equipment. Aside from reinstallation of a smaller beam pipe downstream of the scattering chamber, it puts no unusual demands on the Hall C hardware or the accelerator. It makes use of hydrogen and deuterium targets, the HMS in its current configuration, and beam energies already attained.

References

[Abt93] Abt *et al.*, Nuc. Phys. **B407**, 515 (1993).

[Ada96a] M. R. Adams *et al.*, Phys. Rev. D **54**, 96 (1996).

[Ada96b] M. R. Adams *et al.*, Phys. Rev. D **54**, 3006 (1996).

[Adl97] C. Adloff *et al.*, Nuc. Phys. **B497**, 3 (1997).

[Ahm95] Ahmed *et al.*, Nuc. Phys. **B439**, 471 (1995).

[Aid96] S. Aid *et al.*, Nuc. Phys. **B470**, 3 (1996).

[Arn95] M. Arneodo *et al.*, Phys. Lett. B **364**, 107 (1995).

[Arn97] M. Arneodo *et al.*, Nuc. Phys. **B483**, 3 (1997).

[Blo70] E. D. Bloom and F. J. Gilman, Phys. Rev. Lett. **25**, 1140 (1970).

[Blo71] E. D. Bloom and F. J. Gilman, Phys. Rev. D **4**, 2901 (1971).

[Bre97] J. Breitweg *et al.*, Phys. Lett. B **407**, 432 (1997).

[Bre98] J. Breitweg *et al.*, e-print hep-ph/9809005 (1998).

[Car90] C. E. Carlson and N. C. Mukhopadhyay, Phys. Rev. D **41**, 2343 (1990).

[Cas98] C. Caso *et al.*, The European Physical Journal **C3** (1998) 1.

[Der93] M. Derrick *et al.*, Phys. Lett. B **316**, 412 (1993).

[Der95a] M. Derrick *et al.*, Z. Phys. **C65**, 379 (1995).

[Der95b] M. Derrick *et al.*, Z. Phys. **C69**, 607 (1995).

[Der96] M. Derrick *et al.*, Z. Phys. **C72**, 399 (1996).

[DeR77a] A. De Rújula, H. Georgi, and H. D. Politzer, Phys. Lett. B **64**, 428 (1977).

[DeR77b] A. De Rújula, H. Georgi, and H. D. Politzer, Annals Phys. **103**, 315 (1977).

[Glu95] M. Glück, E. Reya, and A. Vogt, Z. Phys. **C67** 433(1995).

[Glu98] M. Glück, E. Reya, and A. Vogt, e-print hep-ph/9806404 (1998).

[Lai97] H. L. Lai *et al.*, Phys. Rev. D **55**, 1280 (1997).

[Mar94] A. D. Martin, R. G. Roberts, and W. J. Stirling, Phys. Rev. D **50**, 6734 (1994).

[Nic98] I. Niculescu, dissertation, Hampton University (unpublished) (1998).

[Nic99] I. Niculescu *et al.*, two letters submitted to Phys. Rev. Lett. *Copies of these articles are attached to the proposal.*

[Ste75] S. Stein *et al.*, Phys. Rev. D **12**, 1884 (1975).

Experimental Verification of Quark-Hadron Duality

I. Niculescu,[1] C.S. Armstrong,[2] J. Arrington,[3] K.A. Assamagan,[1] O.K. Baker,[1,5] D.H. Beck,[4] C.W. Bochna,[4] R.D. Carlini,[5] J. Cha,[1] C. Cothran,[6] D.B. Day,[6] J.A. Dunne,[5] D. Dutta,[7] R. Ent,[5] B.W. Filippone,[3] V.V. Frolov,[8] H. Gao,[4] D.F. Geesaman,[9] P.L.J. Gueye,[1] W. Hinton,[1] R.J. Holt,[4] H.E. Jackson,[9] C.E. Keppel,[1,5] D.M. Koltenuk,[12] D.J. Mack,[5] D.G. Meekins,[2,5] M.A. Miller,[4] J.H. Mitchell,[5] R.M. Mohring,[10] G. Niculescu,[1] D. Potterveld,[9] J.W. Price,[8] J. Reinhold,[9] R.E. Segel,[7] P. Stoler,[8] L. Tang,[1,5] B.P. Terburg,[4] D. Van Westrum,[11] W.F. Vulcan,[5] S.A. Wood,[5] C. Yan,[5] B. Zeidman[9]

[1] *Hampton University.* [2] *College of William and Mary.* [3] *California Institute of Technology.* [4] *University of Illinois at Urbana-Champaign.* [5] *Thomas Jefferson National Accelerator Facility.* [6] *University of Virginia.* [7] *Northwestern University.* [8] *Rensselaer Polytechnic Institute.* [9] *Argonne National Laboratory.* [10] *University of Maryland.* [11] *University of Colorado at Boulder.* [12] *University of Pennsylvania.*

(December 8, 1999)

A newly-obtained sample of inclusive electron-nucleon scattering data has been analyzed for precision tests of quark-hadron duality. The data are in the nucleon resonance region, and span the range $0.3 < Q^2 < 5.0$ (GeV/c)^2. Duality is observed both in limited and extended regions around the prominent resonance enhancements. Higher twist contributions to the F_2 structure function are found to be small on average, even in the low Q^2 regime of ≈ 0.5 (GeV/c)^2. Using duality, an average scaling curve is obtained. In all cases, duality appears to be a non-trivial property of the nucleon structure function.

The interpretation of the resonance region in inclusive electron-proton scattering and its possible connection with deep inelastic scattering has been a subject of interest for nearly three decades since quark-hadron duality ideas, which successfully described hadron-hadron scattering [1], were first extended to electroproduction. Bloom and Gilman [2] showed that it was possible to equate the nucleon resonance region structure function $\nu W_2(\nu, Q^2)$ (at some typically low Q^2 value) to the structure function F_2 in the deep inelastic regime of electron-quark scattering (at some higher value of Q^2). These structure functions are obtained from inclusive electron-nucleon scattering where the substructure of the nucleon is probed with virtual photons of mass $-Q^2$ and energy ν. The resonance structure function was demonstrated to be equivalent in average to the deep inelastic one, with these averages obtained over the same range in a scaling variable $\omega' = 1 + W^2/Q^2$, where W is the invariant mass. Bloom and Gilman's quark-hadron duality qualitatively explained the data in the range $1 \leq Q^2 \leq 10$ (GeV/c)^2.

This relationship between resonance electroproduction and the scaling behavior observed in deep inelastic scattering suggests a common origin for both phenomena. Inclusive deep inelastic scattering on nucleons is a firmly-established tool for the investigation of the quark-parton model. At large enough values of W and Q^2, Quantum Chromodynamics (QCD) provides a rigorous description of the physics that generates the Q^2 behavior of the nucleon structure function $F_2 = \nu W_2$. The well-known logarithmic scaling violations in the F_2 structure function of the nucleon, predicted by asymptotic freedom, played a crucial role in establishing QCD as the accepted theory of strong interactions [3,4]. However, as Q^2 decreases, the description of the nucleon's structure cannot be expressed in terms of single parton densities with simple logarithmic behavior in Q^2. Inverse power violations in Q^2, physically representing initial and final state interactions between the struck quark and the remnants of the target (termed higher twist effects), must be taken into account as well.

An analysis of the resonance region in terms of QCD was first presented in [5,6], where Bloom and Gilman's approach was re-interpreted, and the integrals of the average scaling curves were equated to the $n = 2$ QCD moments of the F_2 structure function. The Cornwall-Norton moments of the structure function may be expressed as $\int_0^1 x^{n-2} F_2(x) dx$ [7], where $x = Q^2/2M\nu$ is the Bjorken scaling variable, M is the nucleon mass, and n is an integer index. The moments can be expanded, according to the operator product expansion, in powers of $1/Q^2$, and the fall of the resonances along a smooth scaling curve with increasing Q^2 was explained in terms of this QCD twist expansion of the structure function. The conclusion of [5] was that changes in the lower moments of the F_2 structure function due to higher twist effects are small, so that averages of this function over a sufficient range in x at moderate and high Q^2 are approximately the same. Duality is expected to hold so long as $O(1/Q^2)$ or higher inverse power scaling violations are small.

Substantial progress has been made both theoretically in understanding QCD in the past twenty years and experimentally in determining the scaling behavior of the F_2 structure function. Combining the latter with the new precision resonance data presented here [8], it is now possible to revisit quark-hadron duality with a more quantitative approach, addressing the recent theoretical interest in the topic (see, for example, [9–15]).

The data were obtained in Hall C, using the CEBAF

accelerator at Jefferson Lab (JLab). Electron beam energies between 2.4 and 4 GeV, with currents between 20 and 100 μAmps were incident on 4 and 15 ($\pm$ 0.01) cm long liquid hydrogen and deuterium targets. Scattered electrons were detected in both the High Momentum Spectrometer (HMS) and the Short Orbit Spectrometer (SOS), each utilized in a single arm mode to measure the inclusive cross sections.

Nine spectra were obtained for hydrogen and eight for deuterium, covering the invariant mass range $1.0 < W^2 < 4.0$ GeV^2, with central four-momenta in the range $0.3 \leq Q^2 \leq 5.0$ (GeV/c)^2. The structure function $F_2 = \nu W_2$ was extracted from the measured differential cross section σ, using

$$\frac{\sigma \nu Q^4}{4\alpha^2 E'^2} = F_2 \left[\cos^2(\frac{\theta}{2}) + 2\sin^2(\frac{\theta}{2}) \frac{1 + \nu^2/Q^2}{R+1} \right]. \quad (1)$$

Here, α is the fine structure constant, θ is the electron scattering angle, and E' is the scattered electron energy. $R = \sigma_L/\sigma_T$ is the ratio of longitudinal to transverse cross sections. This quantity will be measured at JLab [16], but is currently unknown at the $\pm$100% level in the resonance region for $Q^2 \geq 1$ (GeV/c)^2 [17]. The possible variation of R effects a 2% systematic uncertainty in the extracted F_2 data.

Sample νW_2 spectra extracted from the measured differential cross sections from hydrogen are plotted in Fig. 1 as a function of the Nachtmann scaling variable $\xi = 2x/(1 + \sqrt{1 + 4M^2x^2/Q^2})$. It has been shown that ξ is the correct variable to use in studying QCD scaling violations in the nucleon [18,5]. The arrows indicate $x = 1$ (elastic scattering) kinematics for the four values of Q^2 shown. The solid and dashed curves are from a parameterization [19] of deep inelastic proton structure function data at $Q^2 = 10$ and 5 (GeV/c)^2, respectively. Notice that the resonance spectra at higher (lower) Q^2 appear at higher (lower) ξ on the deep inelastic scaling curve, but that the curve generally represents an average of the data at the disparate kinematics. This is a qualitative manifestation of the original Bloom and Gilman observation.

Because the data were obtained at fixed spectrometer angles, with a few overlapping fixed central momenta, the raw spectra in missing mass (W^2) cover a range in Q^2. The spectra in Fig. 1 have been adjusted to the Q^2 value at $W^2 = 2.5$ GeV^2 for each using a global fit [17] to inclusive resonance region spectra. The difference between the raw and adjused spectra is $\approx$ 3% when integrated. The statistical uncertainty in the data is $\approx$ 1%, smaller than the symbols plotted. The overall systematic uncertainty in the cross sections due to experimental considerations such as target density, beam charge, beam energy, spectrometer acceptance, radiative corrections, detection efficiency, and the value of R, is 3% and is not depicted.

To quantify the observed duality, we show in Fig. 2 the Q^2 dependence of the integral ratio quantity I(Res/DIS), the ratio of the structure function $\nu W_2 = F_2$ obtained from the resonance data, integrated over the region from pion threshold to the onset of the deep inelastic regime ($W^2 = 4$ GeV^2), compared to the indicated deep inelastic structure functions integrated over the same region of ξ:

$$I(Res/DIS) = \frac{\int_{\xi(W^2=4.0)}^{\xi(W^2=1.1)} F_2^{data}(\xi, Q^2 = fixed) d\xi}{\int_{\xi(a)}^{\xi(b)} F_2^{scaling}(\xi, Q^2 = 10) d\xi}. \quad (2)$$

Here, $\xi(a, b)$ correspond to the same value of ξ used in the numerator integral, which at the higher Q^2 of the deep inelastic data no longer correspond to $W^2 = (4.0, 1.1)$, but to some higher $W^2 = (a, b)$. The range $1.1 \leq W^2 \leq 4.0$ GeV^2 is the resonance region of the data. In all cases but the Resonance fit (discussed below), the scaling region structure functions are integrated as a function of ξ at fixed $Q^2 = 10$ (GeV/c)^2. The higher W^2 deep inelastic data are, for the same region in ξ, at higher Q^2. The integral ratio data are plotted as a function of the fixed Q^2 values associated with the measured resonance spectra.

The uncertainties shown represent the experimental uncertainty in the numerator integral only, obtained from the correlated systematic uncertainties in the resonance data. The high Q^2 (above 4 (GeV/c)^2) numerator values are generated from a global fit to inclusive SLAC resonance region data [17] and are assigned an uncertainty representing a combination of experimental uncertainty and normalization considerations involved in utilizing the older data sets [20]. Also shown are very low Q^2 (< 0.5 (GeV/c)^2) resonance data from SLAC [21].

When used to obtain the deep inelastic denominator of the ratios in Fig. 2, the well-known CTEQ4 LQ [22] and MRS(G) LQ [19] scaling curves display a marked deviation from unity which increases with Q^2. This is not necessarily due to higher twist effects, but rather to the difficulty in accurately modeling the large ξ behavior of the structure function. With increasing Q^2, the moments are determined by a smaller and smaller region near $\xi = 1$. Unfortunately, there is a limited amount of deep inelastic F_2 data currently available at large ξ and x and these curves fall below both the average resonance data and the NMC parameterization above $\xi \gtrsim 0.7$.

The points on Fig. 2 labeled NMC represent ratios obtained using a parameterization of lower x deep inelastic F_2 data from CERN [23], which links smoothly to a global fit [20] to higher x deep inelastic data from SLAC, in the denominator integral. Because this is a fit to the data, it may implicitly contain higher twist effects. Using the NMC parameterization, the ratio (Res/DIS) is above unity, but constant at about 1.2. The ratio decreases to about 1.1 when the appropriate logarthmic Q^2 dependence is included to obtain the parameterization at $Q^2 = 5$ (GeV/c)^2. This effect is indicated by the dashed line in the figure.

To obtain the points labeled Resonance fit in Fig. 2, a fit to the *average* strength of *all* the hydrogen resonance spectra was obtained and utilized as a scaling curve. This approach assumes duality, and therefore that the average of the resonance data is equivalent to a proper scaling curve. For small bins in ξ, resonance νW_2 data were averaged, regardless of Q^2, W^2. These average points were then fit as a function of ξ only, and the resultant scaling curve was obtained using a form similar to the x-dependent part of the NMC parameterization [23]. The scaling curve denoted Resonance fit is, then:

$$F_2 = \xi^{0.8699}(1-\xi)^{1.4832}\,[0.2083 - 2.9816(1-\xi) + 17.1260(1-\xi)^2 - 24.1150(1-\xi)^3 + 12.3640(1-\xi)^4]\,. \quad (3)$$

To constrain the fit in the kinematic regions beyond the scope of the data, data obtained from [21] were also used below $Q^2 = 0.5$ (GeV/c)^2 and $\xi = 0.2$. Resonance data in the range $5 < Q^2 < 8$ (GeV/c)^2 were generated from [17] and used to constrain the fit at large ξ. Note that the ratio I(Res/DIS) in Fig. 2 comparing the resonance strength to the Resonance fit scaling curve need not be unity here even though the curve was extracted from the resonance data. The average scaling curve strength at any given value of ξ was obtained from a kinematic range of data at variant values of W^2 and Q^2 oscillating around this curve. The individual spectra used to obtain the plotted ratios are, however, at the indicated fixed Q^2 values only.

The total integrated strength in the region below $W^2 = 4$ GeV^2 averages to values within 10% of the Resonance scaling curve integrated over the same region in ξ, even at Q^2 values as low as ≈ 0.5. Similarly, the ratio I(Res/DIS) is a constant ≈ 1.2, within 10%, when the NMC deep inelastic parameterization is utilized. Additionally, it is indicated that this latter ratio would tend toward unity if it were possible to compare the resonance region data with lower Q^2 values of the deep inelastic. In the QCD-based explanation of duality (e.g. [5]), these results indicate that higher twist effects are surprisingly reduced if the data are integrated over this *full* region. A more stringent test of this reduction of higher twist effects may be found in an analysis of higher order moments due to the greater contribution, at higher n, of larger x, ξ data. In a duality representation, this motivates the need for precision resonance region measurements at higher Q^2 - data which are planned but not yet available [24].

Fig. 3 shows the same duality integral ratio as in Fig. 2, but here obtained more locally, in restricted ξ ranges around the three prominent resonance enhancement regions observed in inclusive nucleon resonance electroproduction, i.e. around the masses of the Δ $P_{33}(1232)$ ($1.3 \le W^2 \le 1.9$ GeV^2), the $S_{11}(1535)$ ($1.9 \le W^2 \le 2.5$ GeV^2), and the $F_{15}(1680)$ ($2.5 \le W^2 \le 3.1$ GeV^2) resonances, and in the higher W^2 region above these ($3.1 \le W^2 \le 3.9$ GeV^2). The uncertainties shown were computed as in Fig. 2. The latter higher mass ratios, which compare near deep inelastic data to deep inelastic data are essentially one and similar to the results in Fig. 2. It has been pointed out [25] that the Δ resonance form factor decreases faster in Q^2 than the leading order perturbative QCD Q^{-4} behavior which the scaling curve should reflect. A similar observation may be made from Fig. 3 where the ratio (Res/DIS) drops below unity in the region $1 < Q^2 < 3.5$ (GeV/c)^2. The S_{11}, on the other hand, appears systematically higher than the others. Generally, however, the lower mass resonances appear to average to the deep inelastic strength, manifesting duality behavior even in these limited ranges of ξ at low Q^2 where higher twist effects might be expected to be large.

By utilizing new inclusive data in the resonance region at large x, it has been possible to revisit quark-hadron duality experimentally for the first time in nearly three decades. These new data, combined with the extensive global measurements of the F_2 structure function from deep inelastic scattering, allow for precision tests of duality in electron-nucleon scattering. The original duality observations are verified, and the QCD moment explanation indicates that higher twist contributions to the $n = 2$ moment of the F_2 structure function are small or cancelling, even in the low Q^2 regime of $Q^2 \approx 0.5$ (GeV/c)^2. Duality is observed to hold for local resonance enhancements individually, as well for the entire $1 \le W^2 \le 4$ GeV^2 resonance region. In all cases, duality appears to be a non-trivial dynamic property of the nucleon structure function.

We acknowledge the outstanding work of the staff of the accelerator division at the Thomas Jefferson National Accelerator Facility. C.E.K. and R.E. wish to thank A. Radyushkin for many useful discussions. This work is supported in part by research grants from the U.S. Department of Energy and the National Science Foundation.

[1] P.D.B. Collins, *An Introduction to Regge Theory and High Energy Physics* (Cambridge University Press, Cambridge, 1977)
[2] E.D. Bloom and F.J. Gilman, Phys. Rev. D **4** (1970) 2901
[3] G. Altarelli, Phys. Rep. **81** (1982) 1
[4] A.J. Buras, Rev. Mod. Phys. **52** (1980) 199
[5] A. De Rujula, H. Georgi, and H.D. Politzer, Ann. Phys. **103** (1977) 315
[6] H. Georgi and H.D. Politzer, Phys. Rev. D **14** (1976) 1829
[7] R. Roberts, *The Structure of the Proton* (Cambridge University Press, Cambridge, 1990)

[8] I. Niculescu, Ph.D. Thesis, Hampton University, 1999
[9] X. Ji and P. Unrau, Phys. Rev. D **52** (1995) 73
[10] V.M. Belyaev and A. Radyushkin, Phys. Lett. B **35** (1995) 194
[11] G. West, hep-ph/9612403 (1996)
[12] G. Ricco *et al.*, Phys. Rev. C **57** (1998) 356
[13] C. Coriano, H-N. Li, and C. Savkli, J. High En. Phys. 9807 (1998) 008
[14] C. Carlson and N. Mukhopadhyay, Phys. Rev. Lett. **74** (1995) 1288
[15] M. Anghinolfi *et al.*, Nucl. Phys. **A602** (1996) 405
[16] Jefferson Lab Experiment E94-110
[17] C. Keppel, Proceedings of the Workshop on CEBAF at Higher Energies, Eds. N. Isgur and P. Stoler (1994) 237
[18] O. Nachtmann, Nucl. Phys. **B63** (1975) 237
[19] A.D. Martin, R.G. Roberts, and W.J. Stirling, Phys. Rev. D **50** (1994) 6734
[20] L.W. Whitlow *et al.*, Phys. Lett. **B282** (1992) 475
[21] S. Stein *et al.*, Phys. Rev. D **12** (1975) 1884
[22] H.L. Lai *et al.*, Phys. Rev. D **55** (1997) 1280
[23] M. Arneodo *et al.*, Phys. Lett. **B364** (1995) 107 (1984) 295
[24] Jefferson Lab Experiment E97-010
[25] P. Stoler, Phys. Rev. Lett. **66** (1991) 1003

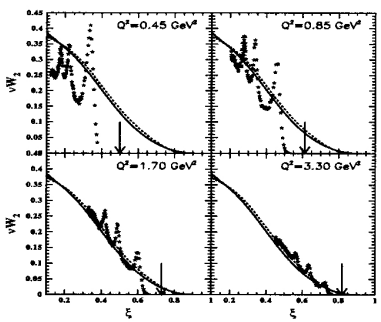

FIG. 1. Sample hydrogen νW_2 structure function spectra obtained at $Q^2 = 0.45, 0.85, 1.70$, and 3.30 (GeV/c)^2 and plotted as a function of the Nachtmann scaling variable ξ. Arrows indicate elastic kinematics. The solid (dashed) line represents the NMC fit [23] of deep inelastic structure function data at $Q^2 = 10$ (GeV/c)^2 ($Q^2 = 5$ (GeV/c)^2).

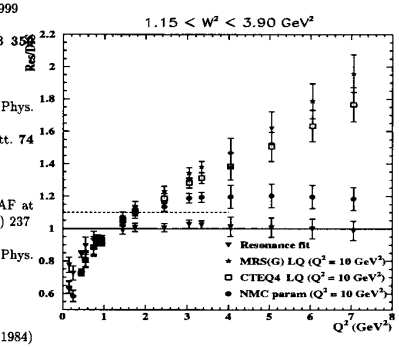

FIG. 2. The ratios of integrals obtained over the hydrogen resonance structure function in the ξ range corresponding to invariant masses between $1.1 < W^2 < 4.0$ GeV^2 (Res) to integrals of the deep inelastic structure functions obtained from parameterizations (stars are Resonance fit; circles are NMC at $Q^2 = 10$ (GeV/c)^2; squares are CTEQ4 low Q^2; triangles are MRS(G) low Q^2) for the same range in ξ (DIS). The dashed line indicates what this ratio would be if the NMC curve were obtained at $Q^2 = 5$ (GeV/c)^2.

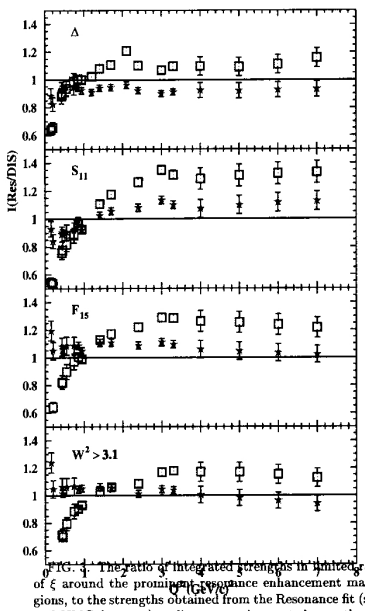

FIG. 4. The ratio of integrated strengths in limited ranges of ξ around the prominent resonance enhancement mass regions, to the strengths obtained from the Resonance fit (stars) and NMC (squares) scaling curves integrated over the same limited ξ regions.

Evidence for Valence-Like Quark-Hadron Duality.

I. Niculescu,[1] C.S. Armstrong,[2] J. Arrington,[3] K.A. Assamagan,[1,5] O.K. Baker,[1,5] D.H. Beck,[4] C.W. Bochna,[4] R.D. Carlini,[5] J. Cha,[1] C. Cothran,[6] D.B. Day,[6] J.A. Dunne,[5] D. Dutta,[7] R. Ent,[5] V.V. Frolov,[8] H. Gao,[4] D.F. Geesaman,[9] P.L.J. Gueye,[1] W. Hinton,[1] R.J. Holt,[4] H.E. Jackson,[9] C.E. Keppel,[1,5] D.M. Koltenuk,[12] D.J. Mack,[5] D.G. Meekins,[2,5] M.A. Miller,[4] J.H. Mitchell,[5] R.M. Mohring,[10] G. Niculescu,[1] D. Potterveld,[9] J.W. Price,[8] J. Reinhold,[9] R.E. Segel,[7] P. Stoler,[8] L. Tang,[1,5] B.P. Terburg,[4] D. Van Westrum,[11] W.F. Vulcan,[5] S.A. Wood,[5] C. Yan,[5] B. Zeidman[9]

[1] *Hampton University.* [2] *College of William and Mary.* [3] *California Institute of Technology.* [4] *University of Illinois at Urbana-Champaign.* [5] *Thomas Jefferson National Accelerator Facility.* [6] *University of Virginia.* [7] *Northwestern University.* [8] *Rensselaer Polytechnic Institute.* [9] *Argonne National Laboratory.* [10] *University of Maryland.* [11] *University of Colorado at Boulder.* [12] *University of Pennsylvania.*

(December 1, 1999)

A newly obtained data sample of inclusive electron-nucleon scattering from both hydrogen and deuterium targets is analyzed. These JLab data are in the nucleon resonance region up to four-momentum transfers of 5 (GeV/c)^2. The data are in agreement with SLAC data at similar kinematics, and are found to follow an average scaling curve. The inclusion of low-momentum transfer data yields a scaling curve resembling deep inelastic neutrino-nucleus scattering data, suggesting a sensitivity to valence-like structure only.

Nearly thirty years ago Bloom and Gilman observed that the electroproduction of resonances resembles the scaling behavior of the deep inelastic structure function, if expressed in terms of a scaling variable connecting the two different kinematic regions, and if averaged over a large range of invariant mass W [1]. It was suggested that this relationship between resonance electroproduction and the scaling behavior observed in deep inelastic scattering hinted at a common origin for both phenomena, called local duality. A quantitative Quantum Chromodynamics (QCD) analysis of this empirical observation was given by De Rujula, Georgi, and Politzer [2]. They showed that the resonances oscillate around an *average* scaling curve. Although electroproduction of resonances is a strongly non-perturbative phenomenenon, the resonance strengths average to a global scaling curve, resembling the deep inelastic scaling curve, as the higher-twist effects are not large, if averaged over a large kinematic region.

Higher-twist effects can be viewed as processes where the struck quark communicates with one or more of the spectator quarks by gluon exchange. In the deep inelastic F_2 data, higher-twist terms have been found to be small for Bjorken $x < 0.40$ [3], and insignificant for $x \approx 0.01$, even at $Q^2 \simeq 1$ (GeV/c)^2, where Q is the four-momentum transfer [4,5]. On the other hand, gauge invariance requires F_2 to vanish linearly with Q^2 at $Q^2 = 0$ (GeV/c)^2 [6], suggesting non-perturbative effects govern this region. In this Letter we assume higher-twist effects, if averaged over the full resonance region, to be small, even at relatively low momentum transfers, and thus local duality to remain valid. A quantitative verification of this assumption will be presented elsewhere [7].

A sample of high-precision data in the nucleon resonance region, in combination with substantial progress made over the last twenty years in determining the scaling behavior of deep inelastic structure functions with electron, muon, and neutrino probes, enables us to revisit local duality in detail. We investigate the connection between resonance electroproduction and deep inelastic scattering to lower four-momentum transfers than previously investigated, and consider possible implications.

We accumulated data in the nucleon resonance region, $1 < W^2 < 4$ (GeV/c)^2, for both hydrogen and deuterium targets [8]. Measurements in the elastic region were included in the data to verify our absolute normalizations to better than 2%. The data were obtained in Hall C at Jefferson Lab (JLab), using electron beam energies between 2.4 and 4 GeV. Incident beam currents between 20 and 100 μA were used on 4 and 15 cm long targets. Scattered electrons were detected in both the High Momentum Spectrometer (HMS) and the Short Orbit Spectrometer (SOS) [8], each utilized in a single arm mode to measure the inclusive cross sections. At all beam energy-scattering angle combinations, the central momentum of the spectrometers was varied to cover the full resonance region. The change in central momentum was kept smaller than the momentum acceptance of each spectrometer, to ensure that overlapping data were accumulated. The internal consistency of the data, within a 16% momentum acceptance for HMS and a 30% momentum acceptance for SOS, was found to be always better than 3%. The Q^2 range covered by our data set is between 0.3 and 5 (GeV/c)^2. We accumulated of order 10^5 counts for every beam energy-scattering angle combination (9 in total for hydrogen, 8 for deuterium). In all cases, the overall systematic uncertainty in the measured cross sections due to target density, beam charge, beam energy, spectrometer acceptance, radiative corrections,

and detection efficiency is less than 3% and larger than the statistical uncertainties [8–10].

We extracted the structure function F_2 from the measured differential cross sections $\sigma = \frac{d^2\sigma}{d\Omega dE_{\prime}}$ like $F_2 \sim \sigma \times (1+R)/(1+\epsilon R)$ [11]. Here ϵ is the virtual-photon polarization and R is the ratio of longitudinal to transverse cross sections. We used a value of $R = 0.2$ for the present analysis, but the results are consistent within 2% if a parametrization of this quantity based on deep inelastic scattering data at moderate Q^2 is utilized [12]. However, we note that this quantity is presently only known at the $\pm 100\%$ level in the nucleon resonance region above $Q^2 \approx 1$ (GeV/c)^2.

A sample of the extracted F_2 data in the nucleon resonance region are shown in Fig. 1a for the hydrogen target, and in Fig. 1b for the deuterium target, as functions of the Nachtmann scaling variable ξ. These figures also include some low Q^2 data from SLAC [13,14]. In terms of the Nachtmann variable $\xi = 2x/(1+\sqrt{1+4M^2x^2/Q^2})$ [15], where M is the nucleon mass, a pattern of scaling violations has been formulated within a QCD framework [2]. The variable ξ takes target-mass corrections into account, necessary as the quarks can not be treated as massless partons for low to moderate momentum transfers. Note that, for low x or large Q^2, the scaling variable ξ is almost identical to the Bjorken scaling variable x.

It is clear from Fig. 1 that indeed the data oscillate around a global curve. This reiterates the well-known local duality picture; the data at various values of Q^2 and W^2 average to a smooth curve if expressed in terms of ξ. For comparison, the solid curve shown represents a global fit to the wold's deep inelastic data [16] for a fixed $Q^2 = 10$ (GeV/c)^2 (NMC10, solid). Previous analyses of local duality have concentrated on a comparison of such deep inelastic constrained curves with nucleon resonance data for $Q^2 \geq 1$ (GeV/c)^2, corresponding to a lower cutoff of $\xi \approx 0.3$. However, as one can see from Fig. 1, the resonance data still seem to oscillate around a global curve, even in the region $\xi \leq 0.3$. This suggests that also in this region the effect of the higher-twist terms is reduced if *averaged* over the full resonance region - consistent with the earlier QCD analysis of the $\xi > 0.3$ region [2]. Note that, for sake of visual clarity, we could not include all of the existing spectra.

From now on we will concentrate on the region of $\xi \leq 0.3$. We initially construct a scaling curve representing the **average** of the resonance data in the region $M^2 \leq W^2 < 4$ (GeV/c)^2, for $Q^2 < 5$ (GeV/c)^2. The average curve for the hydrogen data is shown as a shaded band in Figure 2, where the width of the band takes the systematic uncertainties of the procedure into account. Note that the scaling curve at some ξ value will represent the average of proton resonance data for an extended (W^2, Q^2)-region, but that the average Q^2 will globally increase with ξ. The curves shown represent the global fit to the world's deep inelastic data [16] for a fixed $Q^2 = 10$ (GeV/c)^2 (NMC10, solid), and for a fixed $Q^2 = 2$ (GeV/c)^2 (NMC2, dashed). Whereas the difference between the NMC fit for fixed $Q^2 = 10$ (GeV/c)^2 and $Q^2 = 2$ (GeV/c)^2 is small, and expected from logarithmic scaling violations, the difference between these NMC fits and our data (with $Q^2 \approx 0.3$ (GeV/c)^2) derived from the duality-averaged scaling curve is dramatic at low ξ.

We have used the next-to-leading order calculations of Glück, Reya and Vogt (GRV) [17] to investigate this in more detail. We use the GRV calculations since these are the only ones enabling us to evolute F_2 down to the low momentum transfers of our measurements. In the GRV model, the shape of the gluon and quark-antiquark sea seen by experiment is dynamically generated through gluon bremsstrahlung. The GRV input distribution has been fixed by assuming only valence and valence-like (the input sea quark and gluon distributions also approach zero as $x \to 0$) quark distributions at a finite Q^2 value, constrained with appropriate Q^2-evolutions to deep inelastic F_2 data. We display in Fig. 2 the results of the calculations (GRV, dot-dashed), for Q^2 values close to the average Q^2 of our scaling curve. To compare with the very lowest ξ-region of our data, we also show the *input* distribution itself at $Q^2 = 0.40$ (GeV/c)^2. Note that we here compare data and GRV calculations in a region not advocated by the authors, as "in the very low Q^2 region below 1 (GeV/c)^2 non-perturbative higher-twist contributions are expected to become relevant" [18]. However, as mentioned, our assumption is that the higher-twist effects are reduced, if averaged over the full resonance region. The dotted curve in Fig. 2 denotes the GRV input distribution reflecting *only* the valence quark distributions (i.e. there are no sea quark contributions at all). One can verify that this input distribution is even closer to the actual nucleon-resonance averaged data, at similar Q^2, than the similar input distribution including valence-like effects (dot-dashed curve). The similarity of the various calculations, starting with the mentioned input distributions of Ref. [17], and the average scaling curve given by the nucleon resonance data, suggests that the duality-averaged scaling curve is dominated by valence-quark or valence-like quark contributions.

To verify this, we show in Fig. 3 a comparison of the averaged scaling curve from the deuterium resonance data (solid curve) with a selection of the world's data for the xF_3 structure function. The xF_3 structure function can be accessed by deep inelastic neutrino-iron scattering [19,20], and is associated with the parity-violating term in the hadronic current. Thus, xF_3 measures in the quark-parton model the difference between quark and anti-quark distributions, and is to first order insensitive to sea quark distributions. To enable a direct comparison, we have multiplied our average scaling curve by a factor of 18/5 to account for the quark charges, and have applied a straightforward nuclear correction to the xF_3 data to obtain neutrino-deuterium data [21]. Although

the agreement between the averaged F_2 scaling curve of the deuterium resonance region and the deep inelastic neutrino xF_3 data is not perfect, the similarity is striking. The observation of Bloom and Gilman that there may be a common origin between the electroproduction of resonances and deep inelastic scattering seems to be true for even the lowest values of Q^2 if one assumes sensitivity to a valence-like quark distribution only. Since, at the lowest values of Q^2, one mainly excites the nucleon resonances, and hardly produces inelastic background (corresponding to the non-resonant meson production contributions), one could argue that one just sees the valence-like quarks exciting the various nucleon resonances.

Alternatively, in a parton description, a possible interpretation for the strong Q^2 dependence of F_2 at low ξ and Q^2 could be that, at very low Q^2, the large-wavelength probe is insensitive to coherent quark-antiquark pairs. This interpretation would be at odds with our usual parton description of the perturbative region of deep inelastic scattering, but could transcend the borderline between a parton description and non-perturbative QCD, which we investigate here. In deep inelastic scattering data, which for $\xi \simeq 0.1$ is typically at $Q^2 > 1$ (GeV/c)^2, the sea is indistinguishably intertwined with the the F_2 response. However, at our low Q^2, non-perturbative effects may readily appear in F_2, and are in fact required for $Q^2 \to 0$. The effect is further illustrated in Fig. 4. Here, the shaded bands indicate the range of data and uncertainty in existing high-precision deep inelastic measurements of F_2 [12], at selected values of small x. The solid symbols represent the data extracted from this work, utilizing the averaged proton F_2 scaling curve. The error bars here reflect the range in the x and Q^2 value we use to obtain the scaling curve value at a certain ξ. The open symbols are values of F_2 we extracted from Ref. [14]. These data are measured at invariant masses $W^2 > 4$ (GeV/c)^2, and at low Q^2 values ($Q^2 < 1$ (GeV/c)^2). We have assigned an uncertainty of 8% to these data, reflecting both the uncertainty in our extraction procedure and the normalization uncertainty of these older SLAC data. The data agree well with the shaded band of the more recent high-precision SLAC data. For these x values, the high-W^2, low-Q^2, SLAC data exhibit a Q^2 dependence of the F_2 structure function similar to that observed in our data. The combined data sample allows the conclusion that the observed effect is, to first order, **independent** of the W^2 region.

The solid lines in Fig. 4 are just to guide the eye. We connected our datum at $x = 0.14$ and $Q^2 = 0.3$ (GeV/c)^2 with the SLAC data at similar x and $Q^2 > 0.6$ (GeV/c)^2. For other values of x, the lines have just been offset with the factor multiplying F_2 for various x. The slopes of these lines happen to follow an $F_2 = 0.33\ Q^{0.5}$ behavior. Of course it is likely that we just see an apparent $F_2 \sim Q^{0.5}$ behavior in the limited Q^2 region of our data, transcending the area between scaling at $Q^2 > 1$ (GeV/c)^2 and the $F_2 \sim Q^2$ expectation at $Q^2 \to 0$, based upon gauge invariance [6]. This would be consistent with the rise of deep inelastic F_2 data as a function of Q^2 as shown in Ref. [14]. More data are needed to map the exact Q^2 dependence at low Q^2, to investigate this point in detail. The dashed lines indicate the Q^2 evolution of F_2 starting from the valence-like input distributions of GRV [17,22]. It is clear that the calculations overshoot the low Q^2 data, indicating the presence of a non-perturbative mechanism reducing the measured F_2 structure function. This may be consistent with a turn-on of sensitivity to sea quarks. In contrast, F_2 data extracted from our averaged proton scaling curve at ξ values larger than shown in Fig. 4 (and thus larger Q^2) would be consistent with just a logarithmic Q^2-evolution [8], as can be witnessed in Fig. 2.

In summary, we have measured inclusive electron-nucleon scattering cross sections in the resonance region for both hydrogen and deuterium targets, and have extracted the structure function F_2 from these. The F_2 data oscillate around an average scaling curve, down to the lowest Q^2 measured. The average F_2 scaling curve resembles deep inelastic xF_3 structure function data. Our data suggest that the F_2 structure function at these low momentum transfers follows the behavior of valence-like quarks only. In our kinematics, at intermediate x (~ 0.1) and low Q^2 (~ 0.3 (GeV/c)^2), the structure function F_2 still seems far from following an $F_2 \sim Q^2$ behavior.

We acknowledge the outstanding work of the staff of the accelerator division at the Thomas Jefferson National Accelerator Facility in delivering the high quality electron beam. R.E. and C.E.K. want to thank J. Gomez, N. Isgur, and S. Liuti for helpful discussions. We express gratitude to S. Liuti for a careful reading of the manuscript. This work is supported in part by research grants from the U.S. Department of Energy and the U.S. National Science Foundation.

[1] E.D. Bloom and F.J. Gilman, Phys. Rev. D 4 (1970) 2901; E.D. Bloom and F.J. Gilman, Phys. Rev. Lett. 25 (1970) 1140.
[2] A. DeRujula, H. Georgi, and H.D. Politzer, Phys. Lett. **B64** (1976) 428; A. DeRujula, H. Georgi, and H.D. Politzer, Annals Phys. **103** (1977) 315.
[3] M. Virchaux and A. Milsztajn, Phys. Lett. **B274** (1992) 221.
[4] M. Glück, E. Reya, and A. Vogt, Z. Phys. **C53** (1992) 127.
[5] M. Glück, E. Reya, and A. Vogt, Phys. Lett. **B306** (1993) 391
[6] A. Donnachie and P.V. Landshoff, Z. Phys. **C61** (1994) 139.

[7] I. Niculescu *et al.*, submitted to Phys. Rev. Lett.
[8] I. Niculescu, Ph.D. thesis, Hampton University (1999).
[9] D. Abbott *et al.*, Phys. Rev. Lett. **80** (1998) 5072.
[10] J. Arrington *et al.*, Phys. Rev. Lett. **82** (1999) 2056.
[11] F.E. Close, *An Introduction to Quarks and Partons* (Academic Press, Great Britain, 1979).
[12] L.W. Whitlow *et al.*, Phys. Lett. **B250** (1990) 193.
[13] A. Bodek *et al.*, Phys. Rev. D **20** (1979) 1471.
[14] S. Stein *et al.*, Phys. Rev. D **12** (1975) 1884.
[15] O. Nachtmann, Nucl. Phys. **B63** (1975) 237.
[16] M. Arneodo *et al.*, Phys. Lett. **B364** (1995) 107.
[17] M. Glück, E. Reya, and A. Vogt, Eur. Phys. J. **C5** (1998) 461.
[18] E. Reya, private communications.
[19] P. Berge *et al.*, Z. Phys. **C49** (1991) 187.
[20] E. Oltman *et al.*, Z. Phys. **C53** (1992) 51; J.H. Kim *et al.*, Phys. Rev. Lett. **81** (1998) 3595.
[21] J.J. Aubert *et al.*, Nucl. Phys. **B293** (1987) 740.
[22] S. Liuti, private communications.

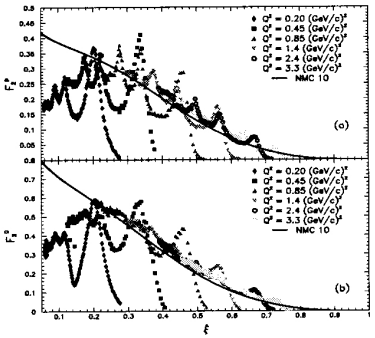

FIG. 1. Extracted F_2 data in the nucleon resonance region for hydrogen (a) and deuterium (b) targets, as functions of the Nachtmann scaling variable ξ. New data from JLab have been extended with high-precision SLAC data. For clarity, only a selection of the data is shown here. The solid curves indicate the result of the NMC fit to deep inelastic data for a fixed $Q^2 = 10$ (GeV/c)^2 [16].

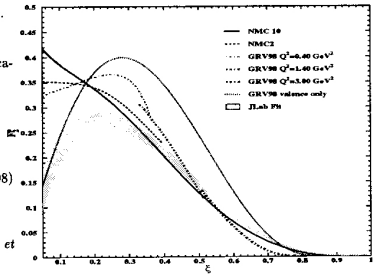

FIG. 2. The shaded band indicates the F_2 scaling curve obtained by averaging over all the proton resonance data (see text). The width indicates the uncertainty in the averaging procedure. The solid curve indicates the result of the NMC fit to deep inelastic data for a fixed $Q^2 = 10$ (GeV/c)^2. The dashed curve shows the result of the NMC fit for a fixed $Q^2 = 2$ (GeV/c)^2. The dot-dashed curves show F_2 obtained from the input valence-like quark distributions (i.e. valence and sea quarks) of Ref. [17], evoluted to Q^2 values close to those of our F_2 scaling curve. Similarly, the dotted curve shows F_2 obtained from the input valence-quark distributions from Ref. [17] only.

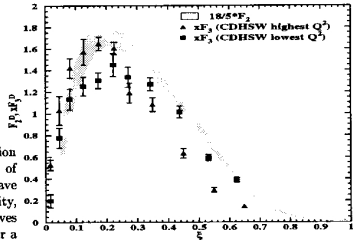

FIG. 3. A comparison of the duality-averaged F_2 scaling curve determined from the nucleon resonance region data with a deuterium target, multiplied by the appropriate factor of 18/5, with the CDHSW data (Ref. [19]) on xF_3 from deep inelastic neutrino-nucleus scattering data, corrected to neutrino-deuterium scattering data. The xF_3 structure function data is to first order sensitive to valence quarks only.

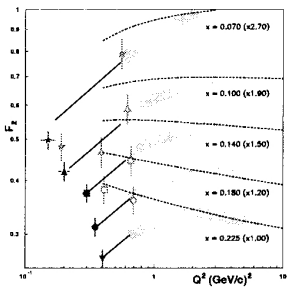

FIG. 4. The low-Q^2 F_2 structure function data for a region in Bjorken x between 0.05 and 0.25. The shaded bands indicate the behavior of the high-precision deep inelastic data from Ref. [12]. The closed symbols represent data extracted from the averaged F_2 scaling curve of the proton resonance region. The open symbols represent data extracted from Ref. [14], with $W^2 > 4$ (GeV/c)^2. Stars, triangles, squares, circles, and inverted triangles represent data at $x = 0.070$, 0.100, 0.140, 0.180, and 0.225, respectively. The solid curves are to guide the eye only and represent a $F_2 \sim 0.33\ Q^{0.5}$ behavior. The dashed curves denote the Q^2-evolution of F_2 starting with the valence-like input distributions from Ref. [17].